

## Physical model simulations of effects of joint spacing and joint angle on rock slope stability

MatseeKleepemk, DechoPhueakphum and KittitepFuenkajorn

Geomechanics Research Unit, Institute of Engineering, Suranaree University of Technology,

Muang District, NakhonRatchasima, Thailand 30000.

Phone (66-44) 223-363, Fax (66-44) 224-448

E-Mail: kittitep@sut.ac.th

### Abstract

Scaled-down physical models are used to simulate slope failure formed by jointed rock mass. The test results are compared with those obtained from the Hoek and Bray's solution, simplified Bishop method and UDEC simulations. A vertical test frame is used to induce slope failure under real gravitational force in two-dimension. Rectangular and parallelepiped blocks of sandstone are saw cut to obtain nominal sizes of 4×4×8 cm, 4×4×12 cm, and 4×4×16 cm to assess the effects of joint spacing and joint angle. The heights of the slope models vary from 0.1 to 1 m and the slope face angles from 14° to 55°. Results indicate that plane sliding occurs when the slopes are gentle and low with large joint spacing while combination of circular and plane sliding modes is obtained when the slopes are steep and high with small joint spacing. The maximum slope height also decreases as the sliding plane angle and slope face angle increase. The slope models with joint dipping into the slope face tend to be less stable than those with the joint dipping away from the slope face. The simulation results well agree with those of the UDEC analyses. Both Hoek and Bray and simplified Bishop solutions however overestimate the stability of the slope models for all joint conditions.

### 1. Introductions

Scaled-down physical models have long been used to simulate the failure behaviour of rock slope in the laboratory [1-3]. They have been used as teaching and research tools to reveal the two-dimensional failure process of rock slopes under

various geological characteristics. They are sometimes employed to gain an understanding of a unique failure process under site-specific conditions. Perhaps the most popular and widely used model is the Goodman's friction table [4]. Bray and Goodman [5] discuss the base friction principle that it is used widely to reproduce the effects of gravity in two dimensional physical models of excavations in rock. They develop mathematical principles upon which analogy between gravity and base friction can be examined. It is claimed that the equations of motion in the realm of the model are obtainable from those of the real world by replacing any linear or angular acceleration term by corresponding linear or angular velocity term. For limiting equilibrium analysis, in which motion is incipient, the analogy is flawless. The friction table has been evolved into several versions. Cement mixed with sand, plaster or wooden blocks are commonly used to form the slope models. Teme [6] has used inclinable base-friction table as a tool in modeling of excavations. It is similar to that described by Goodman [4], Hoek and Bray [7] and Hittinger [8]. Teme's machine can however be inclined to simulate various dip angles in the field, and can test rigid and non-rigid model materials, or both. Recently numerical analyses, primarily with discrete element methods, have been employed to simulate the plane sliding and toppling failures observed from the slope models [9-10]. Comparisons of the results from the computations and observations are made to verify the representative capability of the computer modeling and to improve an understanding of the actual behavior of rock slope failure.

This study involves simulation of the failure of jointed rock slope using scaled-down physical model in the laboratory to assess the effects of joint spacing, joint angle and slope height. The results from the model simulations are compared with those obtained from the deterministic methods and the numerical analyses.

## 2. Test Platform

The test platform used in this study is designed by Pangpetch and Fuenkajorn [1], as shown in Figure 1. The frame is hinged through steel rods in the middle to the stand allowing frame rotation from horizontal position during arranging and loading block samples to vertical position for testing under true gravitational force. When the frame is in horizontal position, the aluminum plate becomes a flat bed supporting the rock blocks during loading. The clear and removable acrylic sheet is installed before rotating the frame to the upright position to prevent the block samples from tipping over. It also allows visual inspection and monitoring of slope movement during the test. The test frame can accommodate 4 cm thick rock blocks arranged to a maximum height of up to 1.5 m to simulate two-dimensional jointed rock slopes. It is designed such that the sliding plane and slope face angles can be continuously increased and monitored during the test until failure occurs.

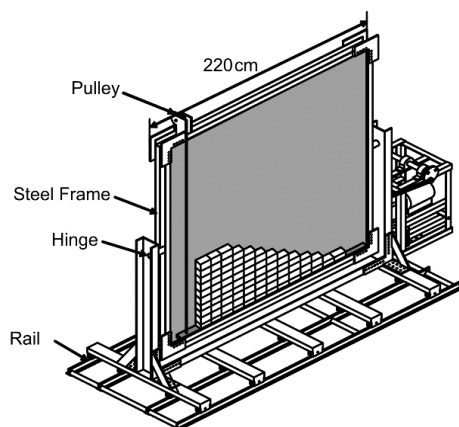


Figure 1 Test frame used in physical model simulation [1].

## 3. Rock Sample

PhuPhan sandstone from NakhonRatchasima province, Thailand has been selected for use as rock sample here primarily because it has highly uniform texture, density and strength. It is classified as fine-grained quartz sandstone with 72% quartz (0.2-0.8 mm), 20% feldspar (0.1-0.8 mm), 3% mica (0.1-0.3 mm), 3% rock fragments (0.5-2mm), and 2% others (0.5-1 mm). The average density is 2.27 g/cc [1]. The slope models are formed by rectangular and parallelepiped blocks of sandstone. Figure 2 shows the rectangular blocks PhuPhan sandstone with dimensions of 4×4×8 cm, 4×4×12 cm and 4×4×16 cm prepared to simulate joint sets with 90° intersection. Parallelogram shaped blocks with dimensions of 4×4×8 cm prepared to simulate joint sets with 135° and 45° intersections. The blocks are prepared by saw-cutting and arranged in the frame to simulate rock slopes with two joint sets having strikes parallel to the slope face. The friction angle of the saw-cutting surfaces of the PhuPhan sandstone determined by tilt testing is 26°. The cohesion obtained from the test is very low (about 0.053 kPa). Over 1000 blocks have been prepared.

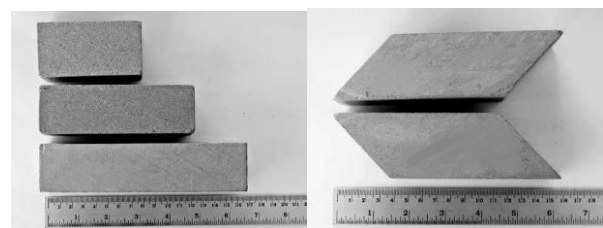
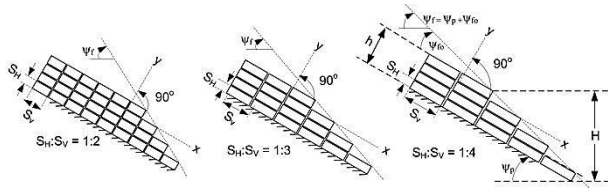


Figure 2 Rectangular blocks of PhuPhansandstone (left). Parallelogram shaped blocks (right).

## 4. Effects of Joint Spacing

Figure 3 shows the block arrangements and geometric parameters of the slope models for assessing the effects of joint spacing. The slope face angles vary from 40° to 51° with the slope height from 16 to 100 cm. The video recorder and visual



**Figure 3** Joint spacing ratios ( $S_H:S_V$ ) vary from 1:2, 1:3 to 1:4 and geometric parameters of the slope models.

observation allows examining the failure process of the slope models during the test. Each slope configuration is simulated three times to ensure correctness of the results. The joint spacing variables are taken as a ratio of the horizontal joint to the vertical joint spacing ( $S_H:S_V$ ). They vary from 1:2 (forming by 4x8 cm blocks), 1:3 (forming by 4x12 cm blocks) to 1:4 (forming by 4x16 cm blocks). Each initial slope face angle ( $\psi_{f0}$ ) of this ratio is 26°, 18° and 14°. The slope height is normalized by the horizontal joint spacing ( $H:S_H$ ) which is varied from 4 to 25. The height of the slope models ( $H$ ) is calculated by the following equation.

$$H = [h \cdot \sin(\psi_{f0} + \psi_p)] / [\sin(\psi_{f0})] \quad (1)$$

where  $h$  is the distance between the base and slope top,  $\psi_{f0}$  is the initial slope face angle, and  $\psi_p$  is the measured sliding plane angle. Table 1 summarizes the test parameters and results for assessing the effects of joint spacing.

**Table 1** Simulation parameters and results for different joint spacing ratios.




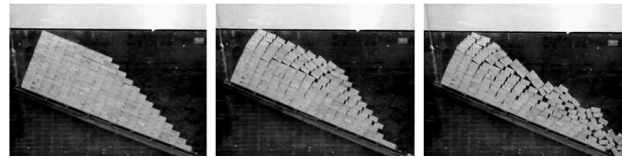
$S_H:S_V$	$\psi_f$ (degrees)	$H/S_H$	$\psi_p$ (degrees)	Failure Modes
1:2 	42-51	5-9	23-25	Plane
		10-25	16-22	Combination
1:3 	40-45	4-12	25-27	Plane
		14-20	22-24	Combination
1:4 	40-44	5-16	24-28	Plane
		17-21	24-26	Combination

Figure 4 shows an example of the failure for a slope model formed by 1:2 joint spacing ratios. Two modes of failures have been observed; plane sliding failures and combination of plane and circular sliding failures. The plane sliding failure occurs under low  $H:S_H$  ratios with high  $S_H:S_V$  ratios while the combination failure is observed under high  $H:S_H$  and low  $S_H:S_V$  ratios.



**Figure 4** Some test results for  $S_H:S_V = 1:2$ , combination failure modes observed.

The simulation results above are compared with the Hoek and Bray's solution [7] for the plane sliding mode and with the simplified Bishop solution [11] for the circular failure. Assuming that the plane sliding mechanism follows the Coulomb criterion, an equation modified from Wyllie and Mah [12] and Kroeger [13] is used to calculate the sliding plane angle, as follows.

$$FS = \frac{c \cdot A + (W \cdot \cos \psi_p) \cdot \tan \phi}{W \cdot \sin \psi_p} \quad (2)$$

where  $c$  is the cohesion of rock surface (equal to 0.053 kN/m<sup>2</sup>),  $\phi$  is the friction angle (equal to 26°),  $\psi_p$  is the inclined sliding plane,  $W$  is the weight of sliding block, and  $A$  is the contact area of the sliding surface.

$$W = \gamma_r \left[ (1 - \cot \psi_f \cdot \tan \psi_p) \left( bH + \frac{1}{2} H^2 \cdot \cot \psi_f \right) + \frac{1}{2} b^2 \left( \tan \psi_s \cdot \tan \psi_p \right) \right] \quad (3)$$

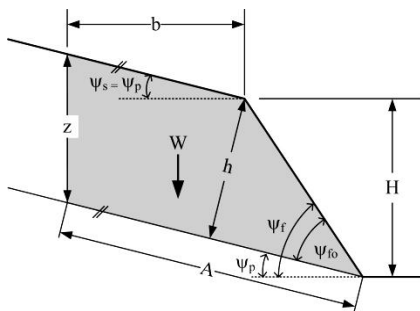
$$A = (H + b \cdot \tan \psi_s \cdot z) \operatorname{cosec} \psi_p \quad (4)$$

$$b = H \sqrt{\cot \psi_f \cdot \cot \psi_p - \cot \psi_s} \quad (5)$$

$$z = H \left[ 1 - \cot \psi_f \cdot \tan \psi_p \right] + b \left[ \tan \psi_s - \tan \psi_p \right] \quad (6)$$

$$H = \frac{z}{1 - \sqrt{\cot \psi_f \cdot \tan \psi_p}} \quad (7)$$

where  $\psi_s$  is the inclined upper slope face,  $\psi_{io}$  is the initial slope face angle,  $\psi_f$  is the slope face angle at failure ( $\psi_f = \psi_{io} + \psi_p$ ),  $\gamma_r$  is the unit weight of rock (equal to  $23.8 \times 10^3 \text{ kN/m}^3$  for PhuPhan sandstone),  $H$  is the slope height at failure,  $b$  is the tension crack location measured from the slope crest, and  $z$  is the vertical tension crack depth. The factor of safety of 1.0 is taken to represent the condition at which failure occurs in the slope models. The parameters used for calculating the contact area of sliding surface ( $A$ ), tension crack location ( $b$ ), slope height ( $H$ ), and tension crack depth ( $z$ ) of Hoek and Bray's solution are shown in Figure 5.



**Figure 5** Parameters of Hoek and Bray's solution (Wyllie and Mah [12] and Kroeger [13]).

Since there is no close-form solution to determine the slope failure under the combination mode, the simplified Bishop method [11-12] is used to define the lower bound of the critical slope height of the test models. The physical model simulations are performed under dry condition. An equation from the simplified Bishop method used here to calculate the factor of safety of a circular failure can be written as follows.

$$FS = [\sum X / (1 + Y / FS)] / \sum Z \tag{8}$$

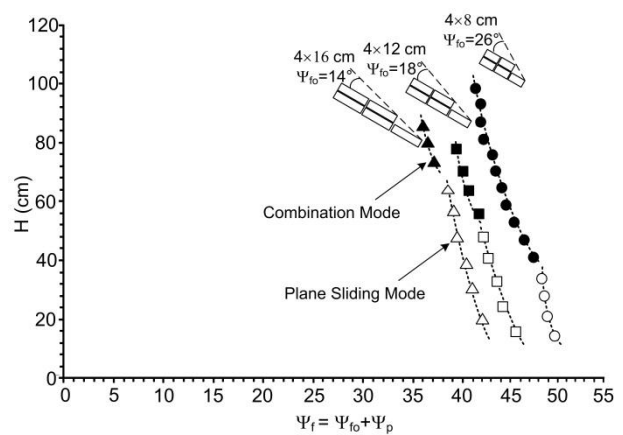
$$X = [c + (\gamma_r \cdot h) \cdot \tan \phi] \cdot [\Delta x / \cos \psi_b] \tag{9}$$

$$Y = \tan \psi_b \cdot \tan \phi \tag{10}$$

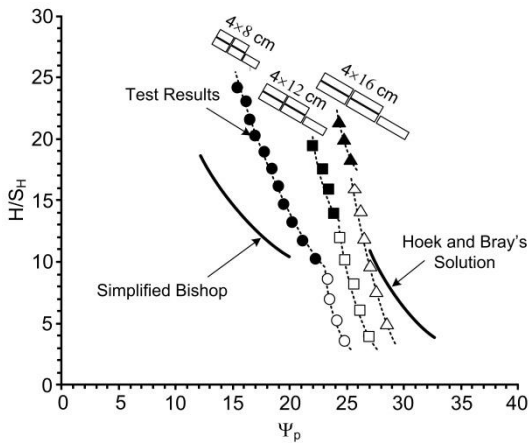
$$Z = \gamma_r \cdot h \cdot \Delta x \cdot \sin \psi_b \tag{11}$$

where  $\Delta x$  are the height and width of each slide,  $X$  and  $Y$  are the coordinates of the center of slipping surface. It is assumed that all slices have the same width. The factor of safety of 1.0 is taken to represent the condition at which failure occurs in the slope models.

The test results in form of the slope height ratio ( $H/S_H$ ) as a function of the slope face angle are presented in Figure 6. Figure 7 compares the calculation results obtained from the two deterministic methods with those of the test models in terms of the slope height ratio as a function of the sliding plane angle. The slope models become more stable as the joint spacing ratio decreases. The transition of the critical slope heights from the pure plane sliding to the combination mode tends to increase as the joint spacing ratio decreases. Under the same sliding angle the Hoek and Bray's prediction gives the critical slope height greater than that of the test models. This suggests that stability analysis using the Hoek and Bray's solution may not be conservative for high slopes formed by jointed rock mass. As expected the simplified Bishop method underestimates the slope height at failure for the combination modes. As the joint spacing ratio increases the differences of the critical slope heights between the Bishop predictions and the test models become smaller.



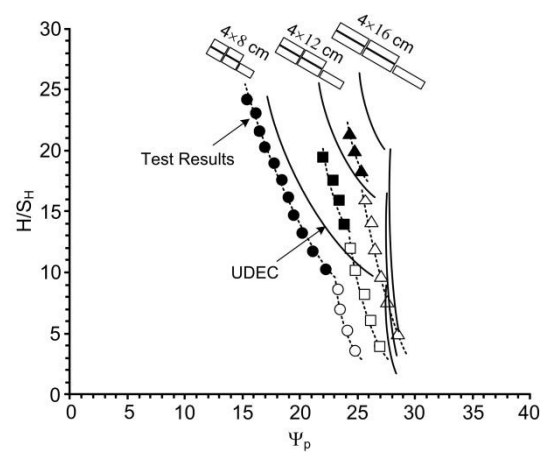
**Figure 6** Test results from studying effects of joint spacing.



**Figure 7** Comparisons between test results and deterministic methods for plane sliding mode (white symbol) and combination mode (solid symbol).

Discrete element analyses are performed using UDEC [14] to describe the stability conditions of the slope models. The discrete element models are constructed to represent various slope geometries and joint spacing as used in the physical model testing. The bulk modulus and shear modulus of the sandstone are calculated from the elastic modulus and Poisson's ratio as 12.3 GPa and 3.8 GPa. The normal and shear joint stiffness values ( $K_n$  and  $K_s$ ) for the smooth joint in PhuPhan sandstone determined by Suanprom [15] are 10 GPa/m and 8 GPa/m, respectively. The joint friction angle and cohesion used in the simulations are  $26^\circ$  and 0.053 kPa. All computer simulations assume plane stress condition. The dilatancy of the joints is assumed to be zero because the surfaces of the tested sandstone blocks are smooth and the cohesion is very low. The corner rounding and the minimum edge length are taken here as 0.001% and 0.002% because the tested sandstone blocks are cubical and rectangular blocks with sharp corners and flat surfaces. Figure 8 compares the UDEC results with the test results in form of the  $H/S_H$  as a function of sliding plane angle ( $\psi_p$ ). The numerical results agree well with the physical model simulations. Two modes of failure are observed from the UDEC results: pure plane sliding and

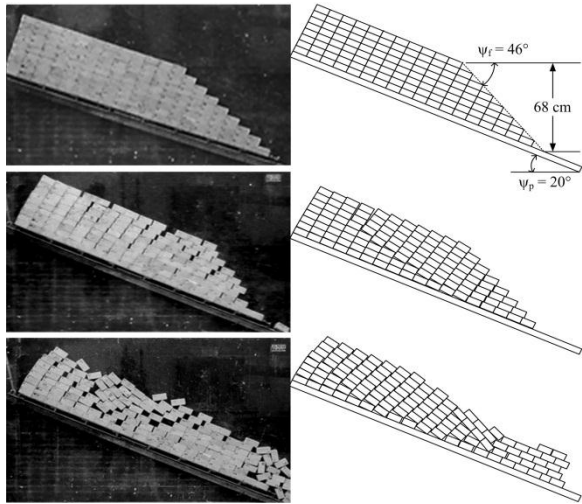
combination of plane sliding and circular failure. The pure plane sliding mode is obtained from low slope heights with high joint spacing ratios. The combination mode occurs for high slopes with low joint spacing ratios. Under the same sliding plane angle the UDEC results tend to show higher critical slope height for combination failure than do the test models. Both UDEC and test models indicate that the slopes comprising large joint spacing ratio (e.g.,  $S_H/S_V = 1:4$ ) tend to fail by plane sliding while those with small joint spacing ratio (e.g.,  $S_H/S_V = 1:2$ ) fail under the combination mode. In addition pure plane sliding failure is observed when the slope models are gentle and low, while combination of plane and circular failures is observed when the slopes are steep and high. Figures 9 compares the physical model with UDEC results for the 4x8 blocks while the failure is in progress. Similar failure sequence is observed from the two methods of simulation. Failure starts near the slope faces and propagates back into the slope mass.



**Figure 8** Comparisons between test results and UDEC analysis.

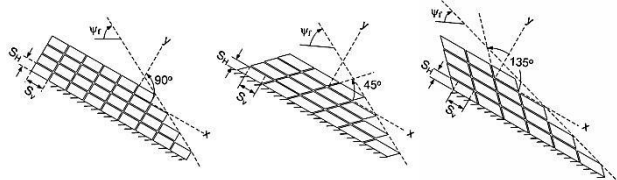
### 5. Effects of Joint Angle

An assessment of the effects of the joint angle on the slope stability has been made by testing the rectangular and parallelepiped blocks with the intersection angles of  $45^\circ$ ,  $90^\circ$



**Figure 9** Comparisons of test observations (left) with UDEC simulations (right) for 4×8 cm block.

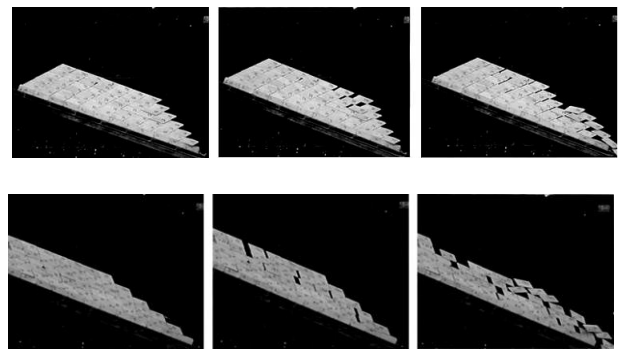
and 135°. The joint spacing ratio of 1:2 is used in these series of simulation (Figure 10). The slope face angle,  $\psi_p$ , vary from 35° to 51°, and slope height, H, from 12 to 100 cm. The height of the slope models (H) is calculated by equation (1). Table 2 summarizes the test parameters and results. Figure 11 gives an example of the failure for a slope model of joint sets with 45° and 135° intersections. Figure 12 compares the critical sliding plane angles observed from the test simulations with those of the simplified Bishop calculation. The combination mode of failure occurs for all slope configurations. The slopes with joints dipping into the slope face are less stable than those with the joints dipping away from the slope face. The simplified Bishop solution underestimates the critical slope height for all cases.



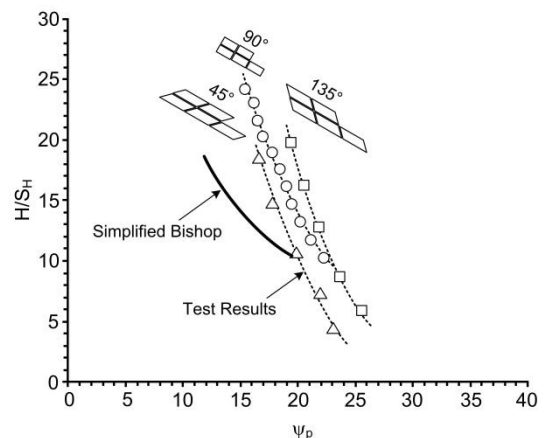
**Figure 10** Parameters used in the simulations of joint angle effects.

**Table 2** Simulation parameters and results for different joint spacing ratios.

Joint set (degrees)	$\psi_f$ (degrees)	H/S <sub>H</sub>	$\psi_p$ (degrees)	Failure Modes
90	42-51	5-9 10-25	23-25 16-22	Plane Combination
135	35-39	5-18	21-25	Combination
45	47-51	3-17	20-24	Combination

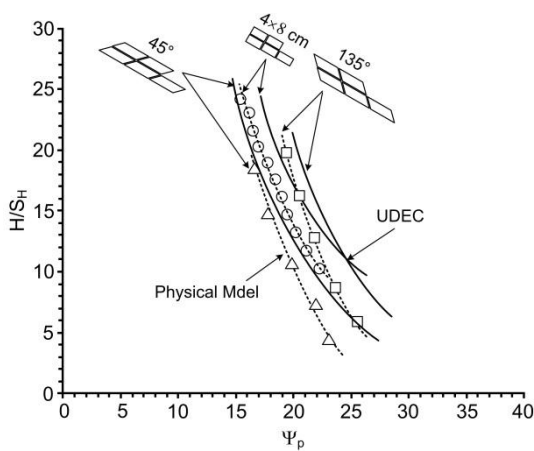


**Figure 11** Some test results for joint set with 45° (top) and 135° (bottom) intersections of plane failure mode.

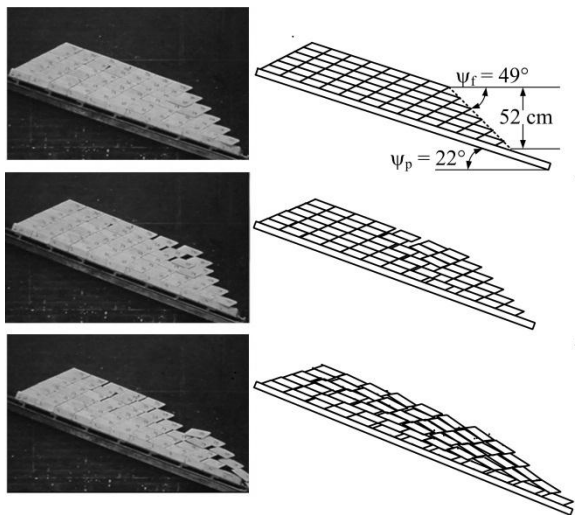


**Figure 12** Comparisons between test results and simplified Bishop solution for combination mode.

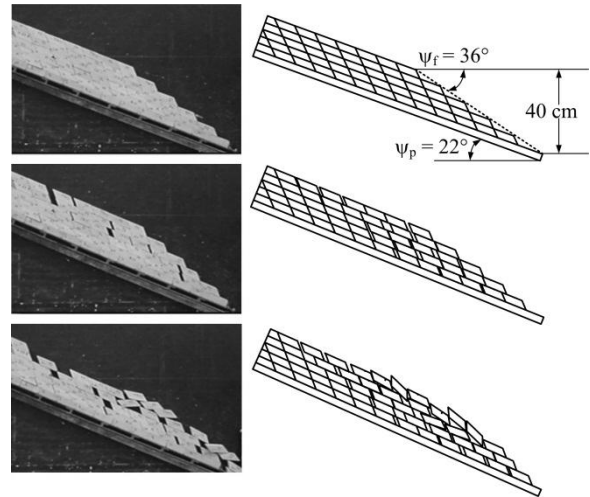
Figure 13 compares the UDEC results with the physical model test results in form of the  $H/S_H$  ratio as a function of  $\psi_p$ . The numerical results agree well with the physical model simulations. Figures 14 and 15 shows the progressive failure of the physical models and the UDEC predictions for joint sets with  $45^\circ$  and  $135^\circ$  intersections while the failure is in progress. Similar failure sequence is observed from the two methods of simulation. Failure starts near the slope faces and propagates back into the slope mass.



**Figure 13** Comparisons between test results and UDEC analysis.



**Figure 14** Test simulation (left) and UDC result (right) for joint set with  $45^\circ$  intersection.



**Figure 15** Test simulation (left) and UDC result (right) for joint set with  $135^\circ$  intersection.

## 6. Discussions and Conclusions

The joints simulated in the slope models here are very smooth and clean with low cohesion and friction angle, which may not truly represent most actual rock joints found under in-situ conditions. The comparisons of the test results with the Hoek and Bray's solution, simplified Bishop's method and UDEC simulations have revealed significant implications that plane sliding dominates when the slopes are gentle and low with large joint spacing (long blocks) while combination of plane and circular sliding is observed when the slopes are steep and high with small joint spacing (shorter blocks). The slope height corresponding to the transition between the two failure modes increases as the joint spacing increases. The maximum slope height also decreases as the sliding plane angle and slope face angle increase. The angle between the intersecting joint set and the sliding joint set also affect of the maximum slope height. The maximum height at failure is greater when the intersecting joints dip away from the slope face (joint set intersection of  $45^\circ$ ) than when they dip toward the slope face (joint set intersection of  $135^\circ$ ). These observations agree reasonably well with the results from the UDEC simulations. The simplified Bishop's method results underestimate the

critical slope height for the combination mode. This is primarily because the solution assumes that the sliding mass is particulate medium. The results suggested that the deterministic method for the combination failure analysis may be conservative for jointed rock slopes. The Hoek and Bray's solution severely overestimates the maximum slope height. The discrepancies increase as the joint spacing decreases. This is primarily because the solution assumes that the sliding block is intact with uniform load applying on the sliding surface. This suggests that the Hoek and Bray's solution may not provide a conservative analysis for slopes with open and small joint spacing.

## 7. Acknowledgements

The work was funded by Suranaree University of Technology. Permission to publish this paper is gratefully acknowledged.

## References

- [1] Pangpetch, P., and Fuenkajorn, K. "Simulation of rock slope failure using physical model," in: Proceedings of the First Thailand Symposium on Rock Mechanics, Suranaree University of Technology, NakhonRatchasima, 2007. pp. 227-243.
- [2] Li, S. H., Wang, J. G., Liu, B. S., and Dong, D. P. "Analysis of critical excavation depth for a jointed rock slope using a Face-to-Face discrete element method," Rock Mechanics and Rock Engineering, 2007. Vol. 40, No.4, pp. 331-348.
- [3] Roy, S., and Mandal, N. "Modes of hill-slope failure under overburden loads: Insights from physical and numerical models," Tectonophysics, 2009. Vol. 473, pp. 324-340.
- [4] Goodman, R. E. "Models of geological engineering in discontinuous rock," West Publishing Company, St Paul, Minnesota, 1976. 562 p.
- [5] Bray, J. W. and Goodman, R. E. "The theory of base friction models," International Journal of Rock Mechanics and Mining Science and Geomechanics, 1987. Vol. 18, No. 6, pp. 453-468.
- [6] Teme, S. C. "A kinematic modeling machine for rock slope studies," International Journal of Mining and Geological Engineering, 1987. Vol. 5, pp. 75-81.
- [7] Hoek, E., and Bray, J. W. Rock slope engineering. 3rd edition, Institute of Mining and Metallurgy, London, 1981.
- [8] Hittinger, M. "Numerical analysis of toppling failures in jointed rock," Ph.D. Thesis, University of California, Berkeley, USA, 1987.
- [9] Kim, Y. G., and Lee, H. K. "Slope stability analysis in discontinuous rocks by base friction model test and its numerical analysis," in: Regional Symposium on Rock Slopes. Coal India Limited, India, 1992. pp. 195-201.
- [10] Lanaro, F., Jing, L., Stephansson, O., and Barla, G. "D.E.M. modeling of laboratory tests of block toppling," International Journal of Rock Mechanics and Mining Sciences, 1997. Vol. 34, No. 3-4, pp. 173-181.
- [11] Bishop, A. W. "The use of the slip circle in the stability analysis of earth slope," Geotechnique, 1995. Vol. 5, pp. 7-17.
- [12] Wyllie, D. C., Mah, C. W. Rock Slope Engineering: Civil and Mining, The Institution of Mining and Metallurgy, London, 2004. 431 p.
- [13] Kroeger, E. B. "Analysis of plane failures in compound slopes," International Journal of Surface Mining, Reclamation and Environment, 2000. Vol. 14, pp. 215-222.
- [14] Itasca, UDEC 4.0 GUI A Graphical User Interface for UDEC. Itasca Consulting Group Inc., Minneapolis, MN, 2004.
- [15] Suanprom, P. "Permeability testing of sheared fractures in sandstones," MS. Thesis, Geotechnology, Suranaree University of Technology, 2009. 78p.